Termodinámica de Superficies

Mezclas

Facultad de Química. Semestre 2020-2

Nombre completo:

Coloque sus repuestas en los espacios correspondientes, digitalice este examen e incluya la hoja donde realizó sus operaciones.

Ejemplo de calculo:

El desarrollo del tema lo puede consultar en la siguiente página **Presión Superficial**

Cálculo de la presión superficial

$$\pi = \sigma_{\text{disolvente}} - \sigma$$

el disolvente es B

$$\pi = \sigma_{\text{B}} - \sigma$$

Tensión superficial de la disolución

Presión superficial de la disolución

x	σ [mN m^{-1}]		x	π [mN m^{-1}]
0	71.8	71.8-71.8	0	0.0
0.01	64.9	71.8-64.9	0.01	6.9
0.30	60.8	71.8-60.8	0.30	11.0
0.50	57.9	71.8-57.9	0.50	13.9
0.60	55.7	71.8-55.7	0.60	16.1
0.70	53.9	71.8-53.9	0.70	17.9
1.00	50.0	71.8-50.0	1.00	21.8

Para más información consulte el siguiente enlace Cálculo de la presión superficial. Si no se encuentra inscrito al curso puede consultar el material en el siguiente enlace Presión superficial (AMyD).

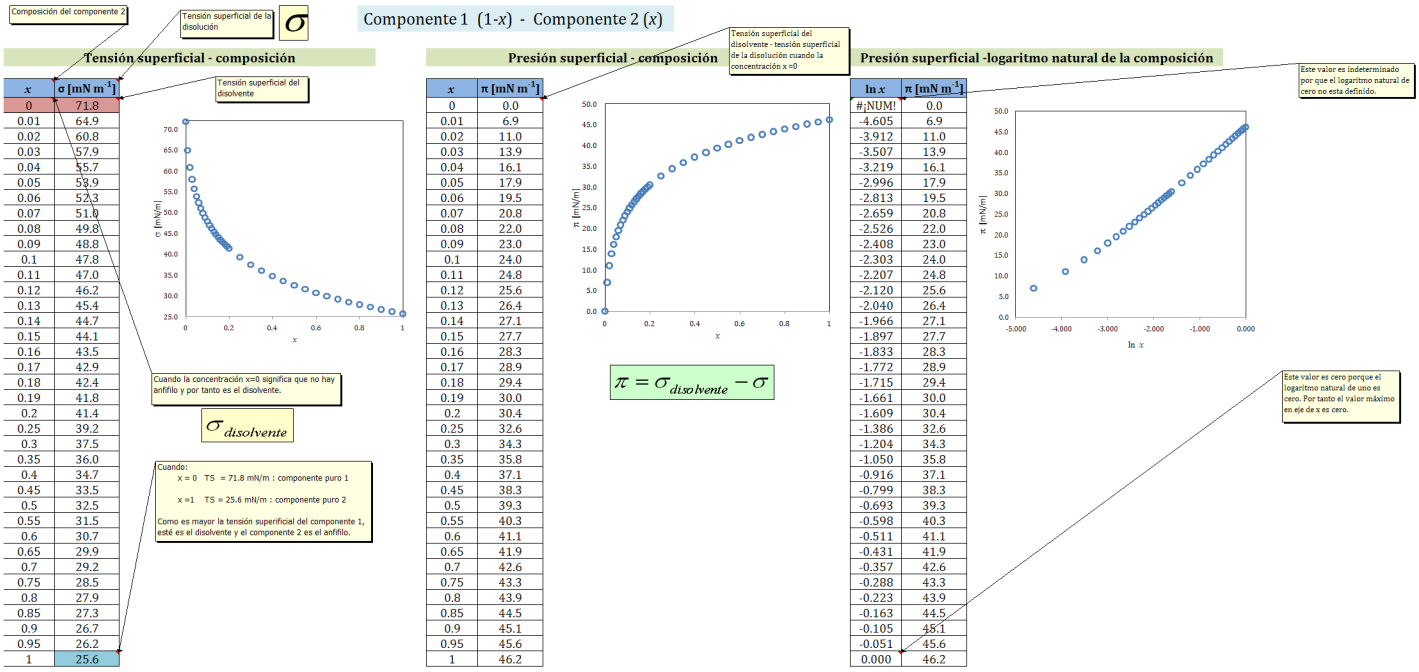

x	σ [mN m^{-1}]
0	71.8
0.01	64.9
0.02	60.8
0.03	57.9
0.04	55.7
0.05	53.9
0.06	52.3
0.07	51.0
0.08	49.8
0.09	48.8
0.1	47.8
0.11	47.0
0.12	46.2
0.13	45.4
0.14	44.7
0.15	44.1
0.16	43.5
0.17	42.9
0.18	42.4
0.19	41.8
0.2	41.4
0.25	39.2
0.3	37.5
0.35	36.0
0.4	34.7
0.45	33.5
0.5	32.5
0.55	31.5
0.6	30.7
0.65	29.9
0.7	29.2
0.75	28.5
0.8	27.9
0.85	27.3
0.9	26.7
0.95	26.2
1	25.6

x	π [mN m^{-1}]
0	0.0
0.01	6.9
0.02	11.0
0.03	13.9
0.04	16.1
0.05	17.9
0.06	19.5
0.07	20.8
0.08	22.0
0.09	23.0
0.1	24.0
0.11	24.8
0.12	25.6
0.13	26.4
0.14	27.1
0.15	27.7
0.16	28.3
0.17	28.9
0.18	29.4
0.19	30.0
0.2	30.4
0.25	32.6
0.3	34.3
0.35	35.8
0.4	37.1
0.45	38.3
0.5	39.3
0.55	40.3
0.6	41.1
0.65	41.9
0.7	42.6
0.75	43.3
0.8	43.9
0.85	44.5
0.9	45.1
0.95	45.6
1	46.2

ln x	π [mN m^{-1}]
#¡NUM!	0.0
-4.605	6.9
-3.912	11.0
-3.507	13.9
-3.219	16.1
-2.996	17.9
-2.813	19.5
-2.659	20.8
-2.526	22.0
-2.408	23.0
-2.303	24.0
-2.207	24.8
-2.120	25.6
-2.040	26.4
-1.966	27.1
-1.897	27.7
-1.833	28.3
-1.772	28.9
-1.715	29.4
-1.661	30.0
-1.609	30.4
-1.386	32.6
-1.204	34.3
-1.050	35.8
-0.916	37.1
-0.799	38.3
-0.693	39.3
-0.598	40.3
-0.511	41.1
-0.431	41.9
-0.357	42.6
-0.288	43.3
-0.223	43.9
-0.163	44.5
-0.105	45.1
-0.051	45.6
0.000	46.2

Figura 1: Hoja de cálculo donde se muestra el cálculo de la presión superficial.La hoja de cálculo la puede descargar en el siguiente enlace Descargar hoja de cálculo o en Descargar hoja de cálculo (AMyD). Además puede ver el video donde se trata de explicar la hoja de cálculo

En la siguiente tabla se muestran datos de tensión superficial en función de la concentración para los sistemas Agua + Etanol, Agua + Metanol y Agua + Propanol. Para cada sistema realice lo siguiente:

1. Identifique al componente que produce la disminución de tensión superficial

2. Con los datos de la tabla, indique el valor de la tensión superficial de los componentes puros.

3. Calcule la presión superficial π para cada composición y debe escribirlos en la tabla para completarla.

4. Elabore un gráfico de la presión superficial π como función de la composición para cada par disolvente-soluto. El gráfico lo debe colocar en la Figura 2. ¡Tenga cuidado con las unidades!.

Agua + Metanol			Etanol + Agua			Agua + Propanol		
x_{agua}	σ[mN/m]	π[mJ/m^2]	x_{etanol}	σ[mN/m]	π[ergio/cm^2]	x_{propanol}	σ[mN/m]	π[dina/cm]
1	72.01		0	72.01		0.000	72.01	
0.971	62.77		0.02	55.73		0.016	41.83	
0.941	56.18		0.042	47.53		0.032	34.32	
0.91	51.17		0.065	42.08		0.050	30.36	
0.877	47.21		0.089	37.97		0.070	27.84	
0.842	43.78		0.115	35.51		0.091	26.64	
0.806	41.09		0.144	32.98		0.114	25.98	
0.727	36.51		0.207	30.16		0.167	25.26	
0.64	32.86		0.281	27.96		0.231	24.80	
0.542	29.83		0.57	26.23		0.310	24.49	
0.432	27.48		0.477	25.01		0.412	24.08	
0.308	25.54		0.61	23.82		0.545	23.86	
0.165	23.93		0.779	22.72		0.730	23.59	
0	22.51		1	21.82		1.00	23.28	

Agua + n-Alcohol

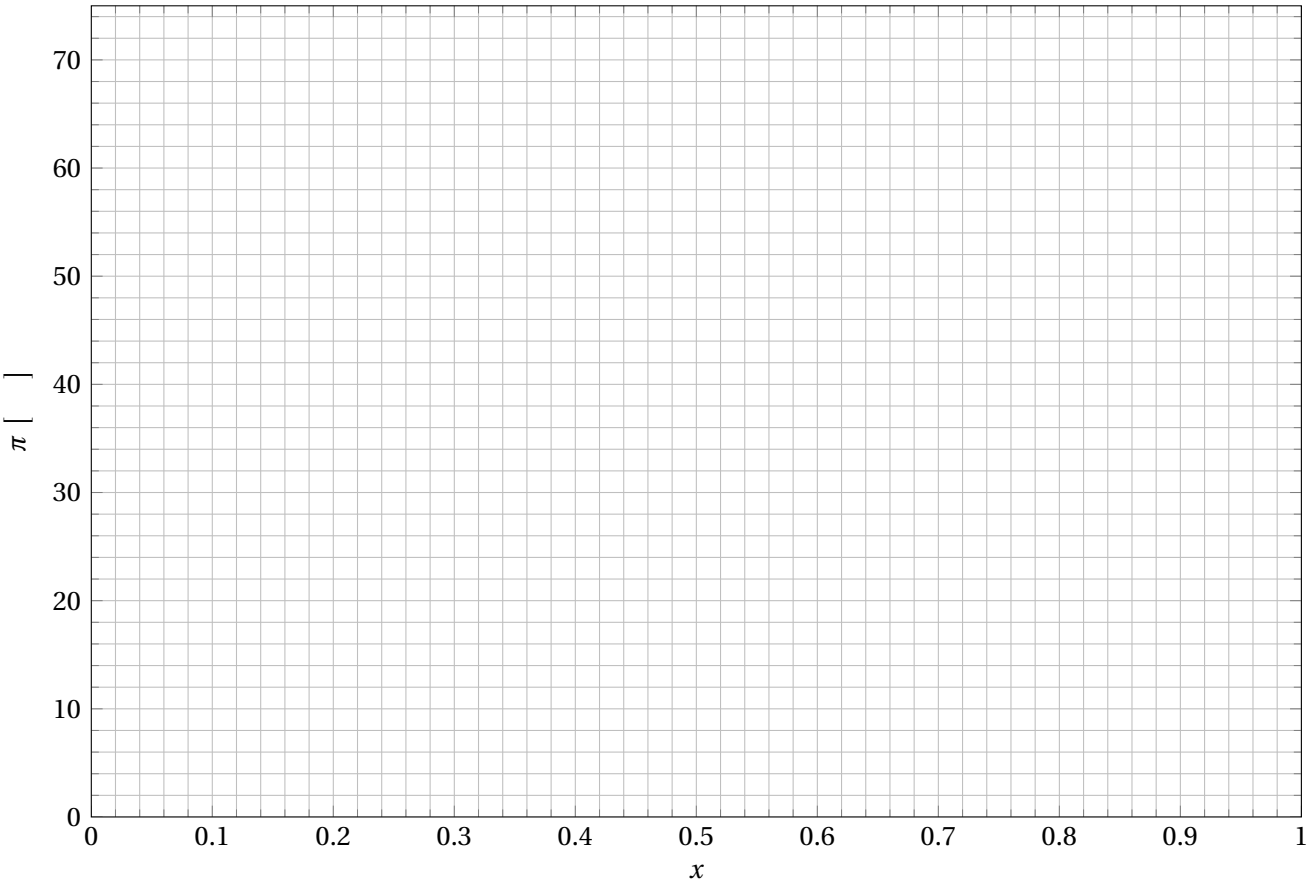

Figura 2: Gráfica presión superficial en función de la concentración.

5. ¿Nota alguna tendencia en relación al número de carbonos en el cadena hidrocarbonada del alcohol?

Y esto ¿sirve de algo?

Leer el **artículo**. ¿Qué es la tensión superficial en exceso? ¿Cómo relacionan la tensión superficial de la disolución con los parámetros moleculares?

Surface tension of water–alcohol mixtures from Monte Carlo simulations

Cite as: J. Chem. Phys. **134**, 044709 (2011); https://doi.org/10.1063/1.3544926
Submitted: 12 November 2010 . Accepted: 04 January 2011 . Published Online: 27 January 2011

F. Biscay, A. Ghoufi, and P. Malfreyt

Surface tension of water–alcohol mixtures from Monte Carlo simulations

F. Biscay,[1] A. Ghoufi,[2] and P. Malfreyt[1,a)]
[1]*Clermont Université, Université Blaise Pascal, Laboratoire de Thermodynamique et Interactions Moléculaires, UMR CNRS 6272, LTIM, BP 10448, F-63000 Clermont-Ferrand, France*
[2]*Institut de Physique de Rennes, UMR CNRS 6251, Université Rennes 1, 263 avenue du Général Leclerc, 35042 Rennes, France*

(Received 12 November 2010; accepted 4 January 2011; published online 27 January 2011)

Monte Carlo simulations are reported to predict the dependence of the surface tension of water–alcohol mixtures on the alcohol concentration. Alcohols are modeled using the anisotropic united atom model recently extended to alcohol molecules. The molecular simulations show a good agreement between the experimental and calculated surface tensions for the water–methanol and water–propanol mixtures. This good agreement with experiments is also established through the comparison of the excess surface tensions. A molecular description of the mixture in terms of density profiles and hydrogen bond profiles is used to interpret the decrease of the surface tension with the alcohol concentration and alcohol chain length. © *2011 American Institute of Physics*. [doi:10.1063/1.3544926]

I. INTRODUCTION

Mixtures of water with alcohols are of fundamental interest in the physical and chemical sciences and also play an important role in numerous engineering applications. Water is a highly structured liquid with a local tetrahedral structure.[1,2] Alcohols, formed by hydrophilic and hydrophobic moities, lead to hydrogen-bonded clusters.[1,2] Mixing water with simple alcohols results in cross associations and in deviations from ideal thermodynamic behavior. The molecular simulations have been developed in the past to investigate the structure of such mixtures.[1–3]

The interfacial tension of these mixtures is also a physical property of great importance for mass transfer such as distillation, extraction, or absorption. The molecular simulation has also been applied for calculating the surface tension of water–methanol mixtures by using a many-body polarizable model for the water–methanol interactions.[4] It is now well-established that the quality of the prediction of the surface tension depends on the methodology used[5] and on the ability of the force field to reproduce accurately the coexisting densities.[6–8]

The methodology for calculating the surface tension of liquid–vapor interfaces of pure molecular systems from a two-phase system is now robust even though a certain number of factors such as the finite size effects,[5,9–11] the range of interactions,[12–15] the truncation effects,[12,16–18] the mechanical and thermodynamic definitions of the surface tension,[6,17,19] and the long range corrections to the surface tension[6,14,16,17,20,21] can impact on the results of this property. Once the methodology was established, molecular simulations of the liquid–vapor interface showed a good reproduction of the temperature dependence of the surface tension for linear and branched alkanes,[7,14,16,17,22] cyclic and aromatic hydrocarbons,[8,23,24] and water and acid gases.[6,25–28] In the case of binary mixtures, the pressure dependence of the interfacial tension was successfully reproduced for methane–water,[29] CO_2–water,[30] and H_2S–water[30] binary mixtures under temperature and pressure conditions close to those encountered in geological storage. These simulations were performed in the Np_NAT ensemble, where p_N is the imposed normal pressure and A the interfacial area.

Concerning the potential used in molecular simulations, the most commonly used is based upon the concept of united atoms (UAs) in which the carbon and its bonded hydrogen are represented by a single force center with the interaction being located at the carbon nucleus. Different UA forcefield OPLS (optimized potential for liquid simulation),[31] SKS (Siepmann–Karaborni–Smit),[32,33] and TraPPE (transferable potentials for phase equilibria)[34,35] have been proposed to predict the phase equilibria of alcohols. Over the past decade, the anisotropic united atom (AUA) initiated by Toxvaerd[36,37] has been successfully applied to different families of hydrocarbons, from linear[38] and branched alkanes,[39] alkenes,[40] and mono- or polyaromatics[24,41–45] compounds. Within the AUA approach, the Lennard-Jones site is offset from the carbon nucleus to be shifted to the hydrogen atoms. It was shown recently[7] that the AUA model allowed efficient predictions of the surface tensions of linear and branched alkanes, whereas the parameters of this force field were not optimized on this property. Recently, an anisotropic united atom intermolecular potential has been derived for the family of alkanols.[46] Good reproductions of the liquid–vapor properties were obtained for a wide variety of primary, secondary, and tertiary alcohols as well as for phenols and diols.[46]

We propose here to study the dependence of the interfacial tension of the liquid–vapor interfaces of water–alcohol mixtures over the entire range of compositions. We focus on the water–methanol, water–propan-1-ol, and water–propan-2-ol mixtures. The water is modeled using the TIP4P/2005 model and the recent AUA4 model[46] is used to represent the alcohols (Table I). All the united atoms involved in the hydrocarbonated part of the alcohol molecules are directly transferred from the AUA4 original model[38] without any

a)Electronic mail: Patrice.Malfreyt@univ-bpclermont.fr.

TABLE I. The Lennard-Jones well depth ϵ and size σ, partial charges q and geometry of alcohol using the AUA4 model (Ref. 46) and of water using the TIP4P/2005 (Ref. 49) model.

AUA4 potential for alcohol[a]				
Atom	ϵ/k_B (K)	σ (Å)	δ (Å)	Charge (e)
CH_3	120.15	3.607	0.216	+0.265 if bonded to O, 0 elsewhere
CH_2	86.29	3.461	0.384	+0.265 if bonded to O, 0 elsewhere
O(OH)	125.01	3.081	0.010	−0.700
H(OH)	0	0	0	+0.435
Bond length	r_0 (Å)			
CH_x–CH_y	1.535			
CH_x–O	1.430			
O–H	0.945			
Bend	θ_0 (°)	k_{bend} (K)		
CH_x–CH_y–O	109.47	59 800		
CH_x–OH	108.5	61 000		
Torsion	a_i (K)			
CH_x–CH_2–O–H	$a_0 = 339.41$	$a_1 = 353.97$	$a_2 = 58.34$	$a_3 = -751.72$
TIP4P/2005 water model[b]				
Atom	σ (Å)	ϵ/k_B (K)	Charge (e)	
O	3.1589	93.2	0	
H	0	0	0.5564	
M	0	0	−1.1128	
OH distance (Å)			0.9572	
H–O–H angle (°)			104.52	
OM distance (Å)			0.1546	

[a]From Ref. 46.
[b]From Ref. 49.

modification. The surface tension of the water–methanol mixture has already been investigated by molecular dynamics simulations[4] where the methanol–water interactions were described by a many-body polarizable potential model.[47,48] The surface tensions calculated here from our Monte Carlo simulations will be compared to these simulations.

The outline of this paper is as follows. In Sec. II, we present the potentials used for water and alcohols. The results and discussions are provided in Sec. III. The main conclusions of this work are summarized in Sec. IV.

II. SIMULATION METHODOLOGY

A. Potential model

Water is modeled using the four-point (TIP4P/2005) model[49] and alcohols are represented by the anisotropic united atom force field AUA4 recently extended to alcohols.[46] The total configurational energy U is defined by

$$U = U_{\text{INTRA}} + U_{\text{INTER}} + U_{\text{LRC}}, \quad (1)$$

where U_{INTRA}, U_{INTER}, and $U_{\text{LRC}}$are the intramolecular, intermolecular, and long range correction (LRC) energy contributions, respectively. The expressions of the different contributions of the intramolecular interactions are given in the supporting information[50] as well as those corresponding to the Lennard-Jones and electrostatic interactions. The long range corrections to the configurational energy are also given for completeness in the supporting information[50] in the case of a multicomponent system.

B. Computational procedures

The simulation box was a rectangular parallelepipedic box of dimensions $L_xL_yL_z$ ($L_x = L_y = 27$ Å, $L_z = 180$ Å) with water and alcohol molecules. Periodic boundary conditions were applied in the three directions. MC simulations were performed in the constant-*NVT* ensemble. Each cycle consisted of N randomly selected moves with fixed probabilities: translation of the center of mass of a random molecule, rotation of a randomly selected molecule around its center of mass, and change of the internal conformation by using the configurational bias regrowth move.[39,51] The frequency of each type of move depends on the mixture considered. For the water–methanol mixture, the occurrences of the various moves are 0.55 for translation and 0.45 for rotation. For the water–propanol mixtures, the occurrences become 0.45 for translation, 0.35 for rotation, and 0.20 for the change of the conformation.

The initial configurations of the water–alcohol interfacial systems were prepared from bulk phase configurations of mixtures of alcohol and water. The initial configurations of alcohol and water were built by placing N molecules on the lattice points of a face-centered cubic structure. The nodes of the lattice where molecules were placed as well as the orientation of these molecules were randomly chosen. The water–alcohol mixtures are modeled at different concentrations from the neat water ($N = 1250$) to neat methanol ($N = 600$) or neat propanol ($N = 350$). The cell parameters of the bulk configurations were set to have the same L_x and L_y dimensions. MC simulations in the NVT ensemble were first performed on the bulk liquid phase of the mixture. The dimension of the

resulting box was increased along the z axis by placing two empty cells on both sides of the bulk liquid box. Some NVT MC steps cycles were carried out to equilibrate the interfacial system. A typical MC run in the NVT ensemble consisted of 300 000 cycles for equilibration and 500 000 cycles for the production phase. Simulations were performed at 298 and 323 K for the water–methanol mixtures and at 298 K for the water–propanol mixtures. Standard deviations of the ensemble averages were calculating by breaking the production runs into block averages. The number of block averages was adjusted in order to allow the convergence of the surface tension within each block.[8] The stability and the independence of the two interfaces are checked through the profiles of the surface tension and the normal and tangential components of the pressure tensor. The constancy of the pseudolocal surface tension $\gamma(z)$ in the bulk regions is also a criterion to check that the configurations are well-equilibrated and that the number of MC cycles is sufficient.

One of the specificities of our MC methodology was the use of the long range corrections to the configurational energy in the Metropolis scheme. The total long range correction energy, U_{LRC}, was updated after each move of molecular position and was added to the energy of the system to be used in the Metropolis scheme.

C. Surface tension

1. Definitions

The most commonly used methods[19,52–56] for the surface tension calculation are based upon the mechanical route definition and use the tensorial components of the pressure. The first explicit form expresses the components of the pressure tensor as a function of the derivative of the intermolecular potential. This operational expression was given by Kirkwood and Buff[53] and is referred here as the KB expression (γ_{KB}). The definition of Irving and Kirkwood[54] (γ_{IK}) is based upon the notion of the force across a unit area and takes advantage of expressing the local components of the pressure tensor along the direction normal to the surface. A novel method based upon the thermodynamic definition of the surface tension (γ_{TA}) has been recently established by Gloor *et al.*[19] and consists in perturbing the cross-sectional area of the system containing the interface. We have also developed a new operational expression of the surface tension based upon the derivative of the potential with respect to the surface.[6] The working expression is referred to KBZ and corresponds to the local version of the KB expression. The long range corrections to the surface tensions induced by the truncation of the Lennard-Jones potential have been developed for each definition in the case of a multicomponent system. The reader is referred to Refs. 29 and 30 for a review about the different derivations of surface tension and the corresponding LRC contributions.

2. System-size checks

It is now well-established that the two-phase simulation[5,9,11,57,58] shows an oscillatory behavior of the calculated surface tension with respect to the interfacial area. The authors have correlated these oscillations to the combined use of periodic boundary conditions and small interfacial areas. Recently,[5] we have demonstrated that the use of LRCs to energy in the Metropolis scheme allows to reduce significantly the oscillatory behavior of the surface

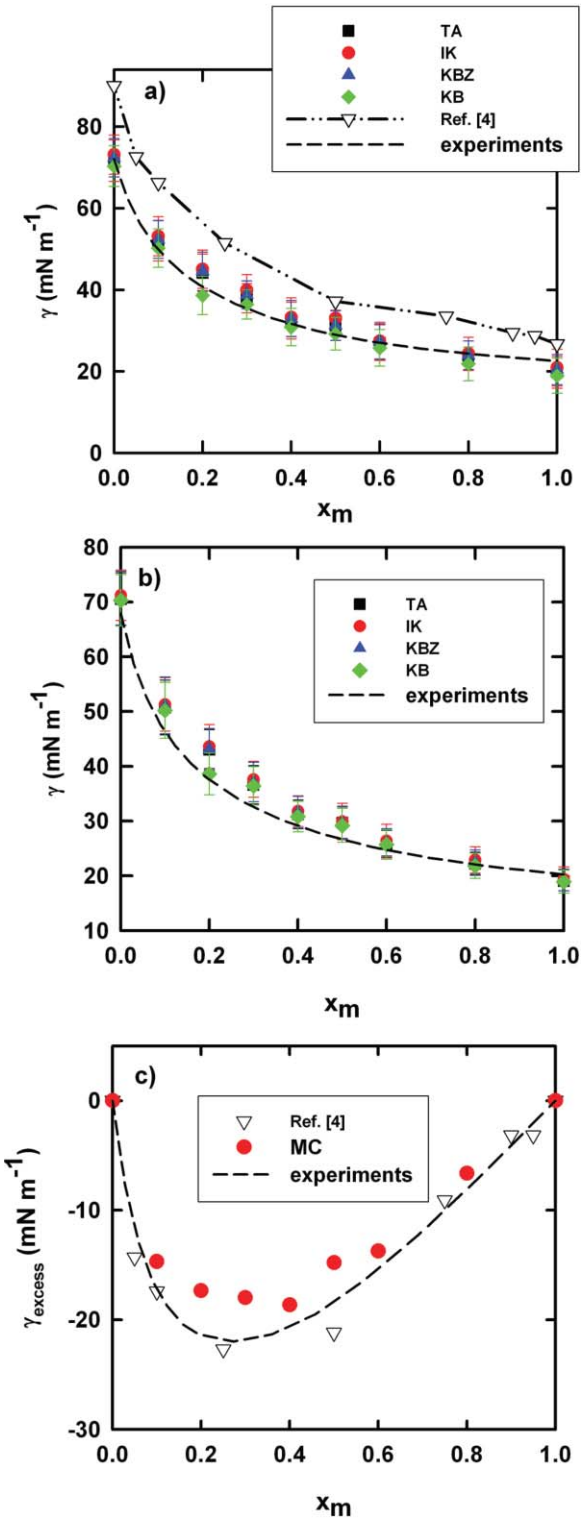

FIG. 1. Interfacial tensions of the water–methanol liquid–vapor interface as a function of the mole fraction x_{m} of methanol at (a) 298 K and (b) 323 K. (c) Excess interfacial tensions of the water–methanol mixture as a function of the composition. We add for comparison the interfacial tensions and excess interfacial tensions calculated from previous molecular dynamics simulations using a polarizable model (Ref. 4).

tension with respect to both the interfacial area and the box dimension in the direction normal to the interface. This strategy of using the LRC contributions to the energy on the fly then allows to use smaller interfacial areas and number of molecules. This aspect was already underlined by Guo and Lu in their original paper.[20] The values of the interfacial areas, used here, correspond to the minimum values from which the oscillatory effects are small with respect to the fluctuations of the surface tension calculation. We have also checked that the surface tension is not dependent on the box dimensions from system sizes used here. These checks confirm those carried in previous simulations of water, CO_2, and H_2S liquid–vapor interfaces with the same interfacial areas.[27]

We have recently concluded[5] that incorporating the LRCs to the energy into the Metropolis scheme and using appropriate LRC expressions for the different definitions of the surface tension result in obtaining cutoff-independent surface tension values whatever the route used for the calculation. This leads us to use a cutoff radius (12 Å) similar to that used for the development of the force field from Gibbs Ensemble Monte Carlo (GEMC) simulations.[46]

III. RESULTS AND DISCUSSIONS

A. Interfacial tensions

The comparison between experimental and simulated interfacial tensions of the water–methanol mixtures is shown in Figs. 1(a) and 1(b) as a function of the methanol mole fraction at 298 and 323 K, respectively. Table II reports the values of the interfacial tensions calculated from the KB, IK, TA, and KBZ definitions. The values of the long range corrections to the surface tensions are also given for completeness as well as the average values calculated over the different definitions. Figure 1(a) shows that the dependence of the calculated interfacial tension of the water–methanol mixture on the methanol mole fraction is very well reproduced with a maximum average deviation of 6.5% with experiments. The interfacial tensions calculated previously using a many-body polarizable potential model[4] show larger deviations that can reach 30% at some methanol concentrations. With this polarizable model, the surface tensions of pure water and pure methanol are significantly overestimated (deviation about 25%). We observe that the change in the interfacial tension is larger at low methanol concentration than at high concentration. A methanol mole fraction of 0.3 is sufficient to decrease the surface tension of water by half. We also observe in Fig. 2(b) that the interfacial tension of the water–methanol mixture is accurately predicted at 323 K for the different concentrations ranging from neat water to neat methanol. The maximum average deviations between simulations and experiments are 5.6%, 8.9%, 7.5%, and 8.2% for the KB, IK, TA, and KBZ routes, respectively. These deviations are slightly larger than those obtained at 298 K. We also reproduce that the interfacial tension of the water–methanol mixture is smaller at 323 K than at 298 K for each methanol composition.

In order to characterize the nonideal behavior of these mixtures, we calculate the excess surface tension γ_{excess} defined by

$$\gamma_{\text{excess}} = \gamma_{\text{w-a}} - (x_{\text{w}}\gamma_{\text{w}} + x_{\text{a}}\gamma_{\text{a}}), \tag{2}$$

where γ_{w} and γ_{a} are the surface tensions of pure water and pure alcohol, respectively, and x_{w} and γ_{a} are the mole

TABLE II. Interfacial tensions (mN m^{-1}) of the water–methanol liquid–vapor interface at 298 and 323 K as a function of the methanol concentration. The long range corrections and the total interfacial tensions are given for each method. $\langle\gamma\rangle$ is averaged over the KB, IK, TA, and KBZ approaches. The experimental interfacial tensions are taken from Ref. 61. The subscripts give the accuracy of the last decimal(s), i.e, 72.1_{50} means 72.1 ± 5.0.

	γ_{KB}		γ_{IK}		γ_{TA}		γ_{KBZ}			
x_{m}	γ_{LRC}	γ	γ_{LRC}	γ	γ_{LRC}	γ	γ_{LRC}	γ	$\langle\gamma\rangle$	$\gamma_{\text{exp.}}$
					$T = 298$ K					
0	3.8_1	71.2_{50}	3.9_1	73.1_{48}	4.3_1	71.6_{51}	4.0_1	72.3_{47}	72.1_{50}	72.0
0.1	3.5_1	51.3_{47}	3.5_1	53.1_{48}	3.9_1	52.0_{50}	3.6_1	52.3_{46}	52.2_{49}	50.7
0.2	3.2_1	43.7_{47}	3.1_1	45.0_{47}	3.4_1	44.1_{46}	3.0_1	44.5_{47}	44.3_{48}	40.7
0.3	2.7_1	37.5_{36}	2.8_1	39.9_{38}	3.0_1	37.9_{36}	2.7_1	38.7_{35}	38.5_{37}	35.3
0.4	2.8_1	32.0_{46}	2.9_1	33.2_{48}	3.1_2	32.4_{45}	2.8_1	32.9_{44}	32.6_{47}	31.5
0.5	2.7_1	29.8_{40}	2.6_1	33.0_{39}	2.9_1	31.2_{37}	2.6_1	31.2_{36}	31.3_{39}	28.9
0.6	2.6_1	27.0_{45}	2.8_1	27.4_{46}	2.9_1	27.0_{44}	2.7_1	27.3_{43}	27.2_{46}	27.0
0.8	2.2_1	23.6_{41}	2.0_1	24.3_{40}	2.4_1	23.8_{36}	2.4_1	23.9_{35}	23.9_{39}	24.3
1	2.3_1	19.6_{43}	2.2_1	20.9_{45}	2.5_1	19.7_{39}	2.3_1	20.4_{37}	20.2_{42}	22.5
					$T = 323$ K					
0.0	5.3_1	70.3_{47}	5.4_1	71.2_{46}	6.0_2	70.5_{48}	5.6_1	70.7_{49}	70.7_{48}	67.9
0.1	4.5_1	50.2_{51}	4.4_1	51.3_{49}	4.8_1	50.7_{50}	4.4_2	51.1_{52}	50.8_{52}	46.9
0.2	3.6_1	38.6_{38}	3.5_1	43.6_{40}	3.8_1	43.0_{37}	3.4_1	43.2_{37}	42.1_{39}	37.5
0.3	3.1_1	36.4_{35}	3.1_1	37.6_{33}	3.1_1	36.6_{35}	3.3_1	37.1_{36}	36.9_{36}	32.5
0.4	2.8_1	30.8_{28}	2.8_1	31.8_{28}	3.2_1	31.2_{26}	3.0_1	31.6_{29}	31.4_{29}	29.0
0.5	2.9_1	29.2_{31}	3.0_1	29.9_{33}	3.1_1	29.7_{29}	2.8_1	29.7_{30}	29.6_{32}	26.6
0.6	2.5_1	25.7_{27}	2.4_1	26.4_{30}	2.7_1	25.8_{25}	2.4_1	26.1_{25}	26.0_{28}	24.8
0.8	2.2_1	21.8_{23}	2.2_1	22.9_{24}	2.5_1	22.2_{21}	1.9_1	22.5_{22}	22.4_{24}	22.0
1.0	2.1_1	18.9_{21}	2.0_1	19.4_{22}	2.4_1	19.0_{22}	2.0_1	19.2_{19}	19.1_{22}	20.2

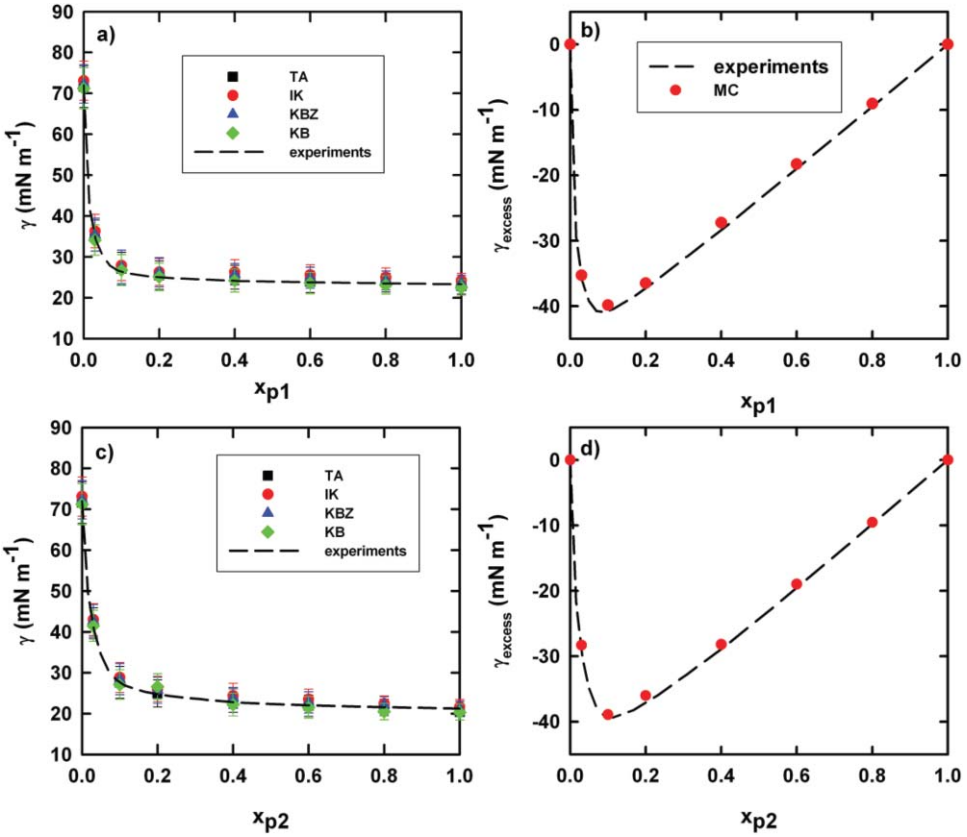

FIG. 2. Interfacial tensions (a) and (c) and excess interfacial tensions (b) and (d) of the water–propanol liquid–vapor interface as a function of the mole fraction x_p of propanol at 298 K for the propan-1-ol and propan-2-ol alcohols.

fractions of water and alcohol. γ_{w-a} is the interfacial tension of the water–alcohol mixture. The excess surface tension is plotted in Fig. 1(c) as a function of the methanol composition at 298 K. The excess surface tensions calculated from our MC simulations are averaged over the KB, IK, TA, and KBZ approaches. We report for the comparison of the excess surface tension calculated from previous molecular dynamics (MD) simulations using a polarizable model.[4] We check that

TABLE III. Interfacial tensions (mN m^{-1}) of the water–propanol liquid–vapor interface at 298 K as a function of the propanol concentration for the primary propanol-1-ol and secondary propan-2-ol. The long range corrections and the total interfacial tensions are given for each method. $\langle\gamma\rangle$ is averaged over the KB, IK, TA, and KBZ approaches. The experimental interfacial tensions are taken from Ref. 61. The subscripts give the accuracy of the last decimal(s), i.e, 27.3_{39} means 27.3 ± 3.9.

	γ_{KB}		γ_{IK}		γ_{TA}		γ_{KBZ}			
x_p	γ_{LRC}	γ	γ_{LRC}	γ	γ_{LRC}	γ	γ_{LRC}	γ	$\langle\gamma\rangle$	$\gamma_{exp.}$
					Water + propan-1-ol					
0.00	3.8_1	71.2_{50}	3.9_1	73.1_{48}	4.3_1	71.6_{51}	4.0_1	72.3_{47}	72.1_{50}	72.0
0.03	3.6_1	34.1_{50}	3.7_1	36.3_{48}	4.1_1	35.2_{51}	3.8_1	35.4_{47}	35.3_{39}	34.3
0.10	3.5_1	26.8_{38}	3.6_1	27.9_{37}	4.1_1	27.1_{40}	3.8_1	27.5_{41}	27.3_{39}	27.0
0.20	3.3_1	25.1_{34}	3.4_1	26.3_{33}	4.0_1	25.5_{35}	3.7_1	26.2_{36}	25.8_{35}	25.1
0.40	2.5_1	24.2_{28}	2.5_1	26.3_{30}	2.9_1	25.0_{29}	2.5_1	25.7_{26}	25.3_{28}	24.4
0.60	2.4_1	23.6_{26}	2.5_1	25.6_{25}	2.8_1	23.9_{26}	2.0_1	24.9_{26}	24.5_{26}	24.0
0.80	2.2_1	23.1_{22}	2.4_1	25.0_{23}	2.5_1	23.7_{26}	2.1_1	24.2_{23}	24.0_{23}	23.7
1.0	2.0_1	22.5_{19}	2.1_1	24.2_{18}	2.2_1	22.9_{20}	2.0_1	23.6_{19}	23.3_{19}	23.3
					Water + propanol-2-ol					
0.0	3.8_1	71.2_{50}	3.9_1	73.1_{48}	4.3_1	71.6_{51}	4.0_1	72.3_{47}	72.1_{50}	72.0
0.03	3.6_1	41.5_{38}	3.7_1	43.0_{39}	4.0_1	42.1_{38}	3.8_1	42.7_{40}	42.3_{39}	40.4
0.10	3.6_1	27.1_{36}	3.6_1	28.8_{37}	3.8_1	27.6_{39}	3.7_1	28.4_{38}	28.0_{39}	29.0
0.20	3.5_1	26.6_{31}	3.7_1	26.0_{31}	3.6_1	24.9_{33}	3.6_1	25.7_{32}	25.8_{31}	24.8
0.40	2.3_1	22.2_{28}	2.4_1	24.4_{28}	2.6_1	23.2_{29}	2.5_1	23.8_{26}	23.5_{28}	23.2
0.60	2.2_1	21.5_{26}	2.1_1	23.5_{26}	2.3_1	21.9_{26}	2.2_1	22.7_{26}	22.4_{26}	22.6
0.80	2.2_1	20.5_{26}	2.1_1	22.4_{24}	2.2_1	21.5_{23}	2.2_1	22.1_{22}	21.6_{23}	22.0
1.0	2.0_1	20.3_{19}	2.1_1	21.6_{19}	2.1_1	20.4_{20}	2.1_1	21.1_{19}	20.9_{19}	21.2

the sensitivity of the water–methanol interfacial tension to the change in the methanol concentration is very well reproduced from our MC simulations. Interestingly, whereas the interfacial tensions calculated from the polarizable model present significant deviations with experiments, the excess interfacial tension is accurately predicted.

We now focus on the calculation of the interfacial tension of the mixtures of water and propanol. Figures 2(a) and 2(c) show the interfacial tension of the mixture at various propanol concentrations with the primary propan-1-ol and the secondary propan-2-ol, respectively. The different interfacial tensions are given in Table III for each method. The maximum deviation between experiments and simulations does not exceed 5%. When the simulated surface tension is averaged over the four methods, the deviation is less than 2%. This constitutes an excellent prediction for this interfacial property. The dependence of the interfacial tension on the alcohol concentration is very pronounced at low propanol amounts. The interfacial tension is reduced by half for the primary propanol and 41% for the secondary propanol at a propanol mole fraction of 0.03. From the mole fraction of 0.1, the interfacial tension of the water–propanol mixture becomes less dependent on the propanol concentration. Because the propanol has a more marked hydrophobic character than the methanol due to its larger alkyl chain, it can cause a deeper decrease of the surface tension at lower alcohol concentration. The average excess interfacial tensions calculated over the different definitions are reported in Figs. 2(b) and 2(d) for the primary and secondary propanols, respectively. The agreement between experimental and simulated excess interfacial tensions is excellent over the entire range of compositions.

Figures 3(a) and 3(b) compare the interfacial tensions and excess interfacial tensions between the water–methanol, water–propan-1-ol, and water–propan-2-ol mixtures at small alcohol concentrations. The simulated surface tensions are averaged over the different definitions. Fig. 3(a) confirms the high ability of propanol to reduce the surface tension of the mixture at very low alcohol concentration and the quality of the reproduction of the surface tension by Monte Carlo simulations. Indeed, the small differences observed between the primary and secondary propanols in Fig. 3(a) are very well predicted by the simulation. The larger differences between methanol and propanol solutions at low alcohol concentrations are also well predicted. The performance of the prediction at low alcohol concentrations has also been extended to the excess surface tension [see Fig. 3(b)]. As expected from the length of the alkyl chain, the deviation from the ideal behavior is much more pronounced for propanol than for methanol.

To summarize, the prediction of the surface tension of the water–methanol and water–propanol mixtures from MC simulations is found to be excellent for all methods used. The change in the water–alcohol interfacial tension with alcohol concentration is found to be accurately reproduced. It means that the water TIP4P/2005 and AUA4 alcohol models show a certain transferability because these models were not developed over this interfacial property. In the remainder of this paper, we give a molecular description of the interfacial and bulk regions.

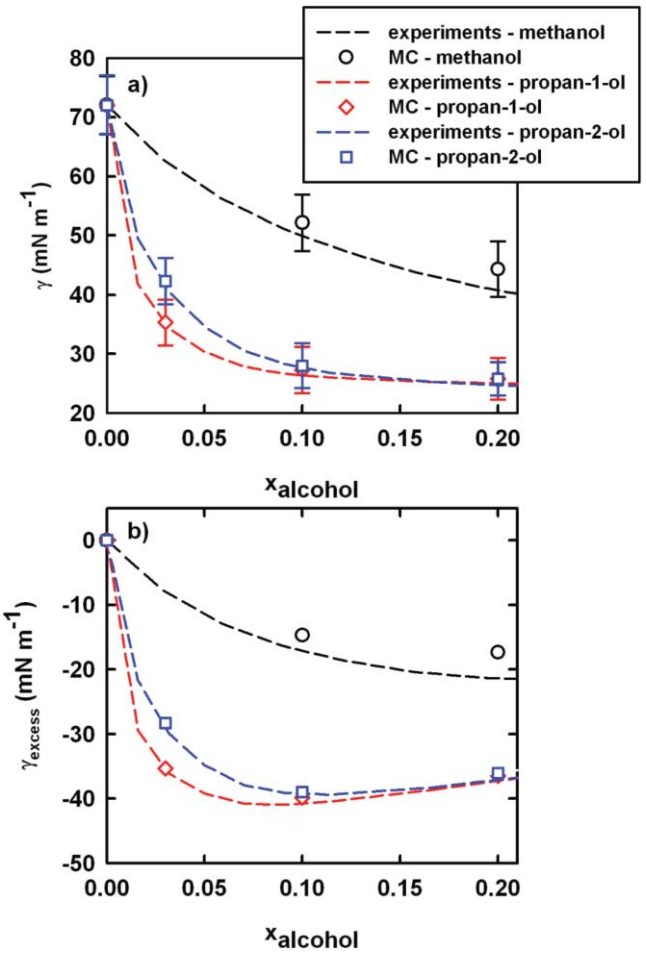

FIG. 3. (a) Interfacial tensions and (b) excess interfacial tensions of the water–alcohol liquid–vapor interface as a function of the mole fraction of alcohol for small alcohol concentrations. The simulated surface tensions are averaged over the IK, TA, KB, and KBZ approaches.

B. Local compositions

The molecular density profiles of the water, methanol, and water + methanol are shown in Fig. 4(a) for a methanol mole fraction of 0.40 at 298 K. These profiles show that the liquid phase is well-developed and covers a region of 50 Å. Figure 4(b) shows the density profiles of the methanol molecules from a pure methanol solution to a very dilute methanol solution. Interestingly, we observe a surface excess of methanol which tends to concentrate at the surface for $x_m < 0.4$. At this concentration, methanol mimics a surfactant and we observe a significant decrease of the water–methanol surface tension (a factor 2 with respect to the surface tension of the pure water). For larger methanol mole fractions, the alcohol molecules are not distributed preferentially any more at the interface and the water–methanol mixture is homogeneously mixed at the molecular level for each z of the bulk liquid phase [see Fig. 4(a)]. The surface tension of the water–methanol mixture decreases slowly with the increasing methanol concentration. At low methanol concentrations, the methanol prefers to adsorb at the interface to favor the hydrophobic interactions with the vapor whereas the high methanol concentrations favor the formation of clusters

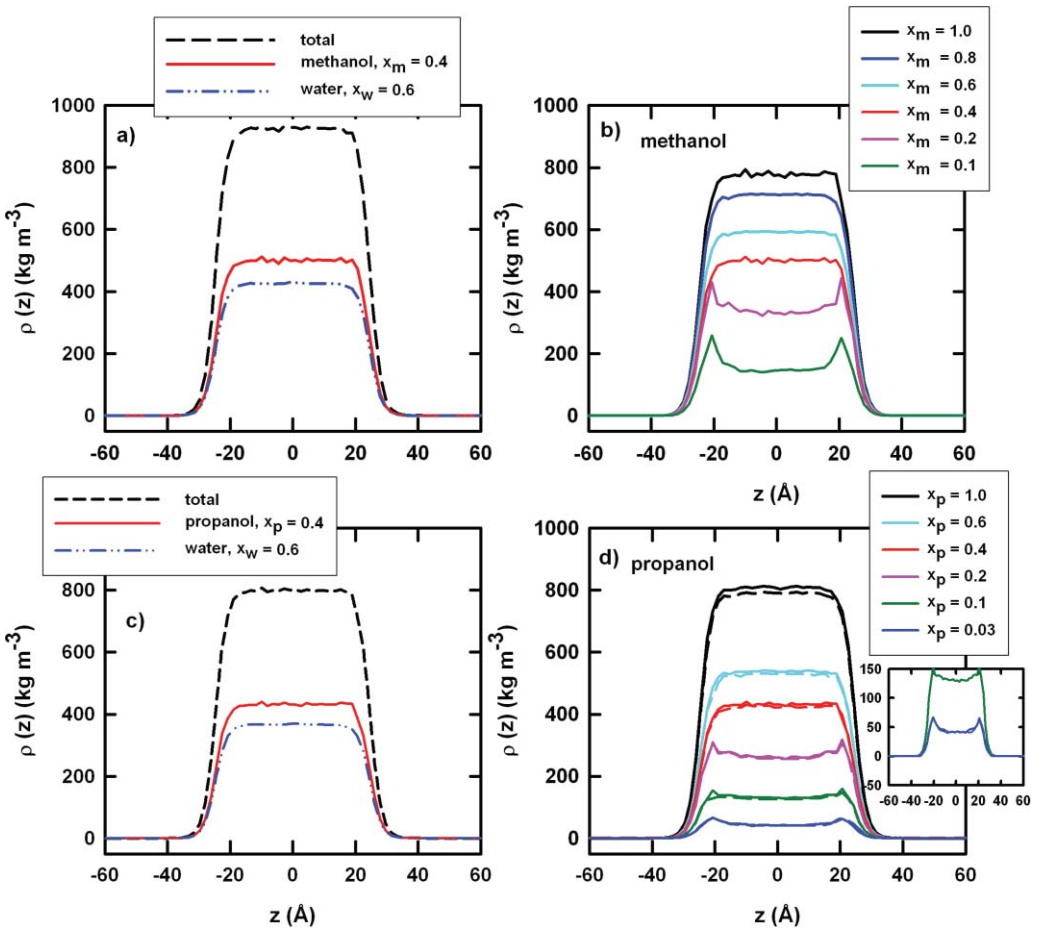

FIG. 4. Molecular density profiles of water, alcohol and water + alcohol for the (a) water–methanol and (c) water–propanol mixtures. (b) methanol density profiles at different methanol mole fractions x_m and (d) propan-1-ol (solid line) and propan-2-ol (dashed line) density profiles at different propanol mole fractions x_p at 298 K.

in the water bulk for which the hydrophobic interactions are predominant.

The density profiles of the water and propan-1-ol are given in Fig. 4(c) for a mole fraction of 0.4. These profiles confirm that the propanol is soluble in water in all proportions and that the mixture is homogeneous for every z of the liquid phase. Figure 4(d) shows local enhancements of the propanol density at the surface relative to the bulk liquid phase for propanol mole fractions lower than 0.2. The inset of Fig. 4(d) underlines these local enhancements by zooming on the profiles of the smallest propanol concentrations. This surface excess is at the origin of the deep decrease of the surface tension as shown for methanol. Actually, the integration of the water and alcohol density profiles at the interfacial region shows that the interfacial region represents alcohol mole fractions of 5% for propan-1-ol and propan-2-ol, whereas the amount of alcohol in the simulation cell is 3%. For an alcohol amount of 0.1, the mole fractions in the interfacial region are 13% and 10% for methanol and propanol, respectively. This confirms that the surface excess at the interfacial region is more pronounced at low propanol concentrations.

C. A link between interfacial tension and hydrogen bonds

A link between the formation of hydrogen bonds network and the Lennard-Jones and electrostatic contributions of the surface tension has already beenestablished from simulations of pure water.[6,59] Table IV reports the decomposition of the interfacial tension into the Lennard-Jones, electrostatic, and long range contributions for various alcohol concentrations. The surface tension of pure water at 298 K calculated from the IK method is 73.1 mN m^{-1} including −63.2 and 132.4 mN m^{-1} for the Lennard-Jones and electrostatic contributions, respectively. The average water–water interaction is then −45 kJ mol^{-1} summing 9 and −54 kJ mol^{-1} for the Lennard-Jones and electrostatic interactions, respectively. As already shown in previous simulations,[6,59] the Lennard-Jones contribution of γ in pure water is negative due to the fact that the hydrogen bonds formed between water molecules lead to strong repulsive oxygen–oxygen Lennard-Jones interactions. In contrast, the surface tension of pure methanol is 20.9 mN m^{-1} at 298 K (Table IV) with a positive Lennard-Jones contribution of 5.6 mN m^{-1} and a positive electrostatic part of

TABLE IV. Contributions of the interfacial tensions (mN m^{-1}) derived from the Lennard-Jones contribution (γ_{LJ}), the electrostatic part γ_{ELEC} calculated using the Ewald summation method and the long range corrections (γ_{LRC}). These contributions are calculated over the whole alcohol concentration range using the IK definition at 298 K.

	γ			
$x_{alcohol}$	γ_{LJ}	γ_{ELEC}	γ_{LRC}	γ_{TOT}
	Water + methanol			
0.0	−63.2	132.4	3.9	73.1
0.10	−55.8	105.4	3.5	53.1
0.20	−52.4	94.3	3.1	45.0
0.30	−40.4	77.5	2.8	39.9
0.40	−38.1	68.4	2.9	33.2
0.50	−22.0	52.4	2.6	33.0
0.60	−6.5	31.1	2.8	27.4
0.80	3.7	18.6	2.0	24.3
1.0	5.6	13.1	2.2	20.9
	Water + propan-1-ol			
0.0	−63.2	132.4	3.9	73.1
0.03	−45.3	77.9	3.7	36.3
0.10	−37.3	61.6	3.6	27.9
0.20	−33.0	55.9	3.4	26.3
0.40	−15.7	39.5	2.5	26.3
0.60	−8.1	31.2	2.5	25.6
0.80	2.3	20.3	2.4	25.0
1.00	4.2	17.9	2.1	24.2

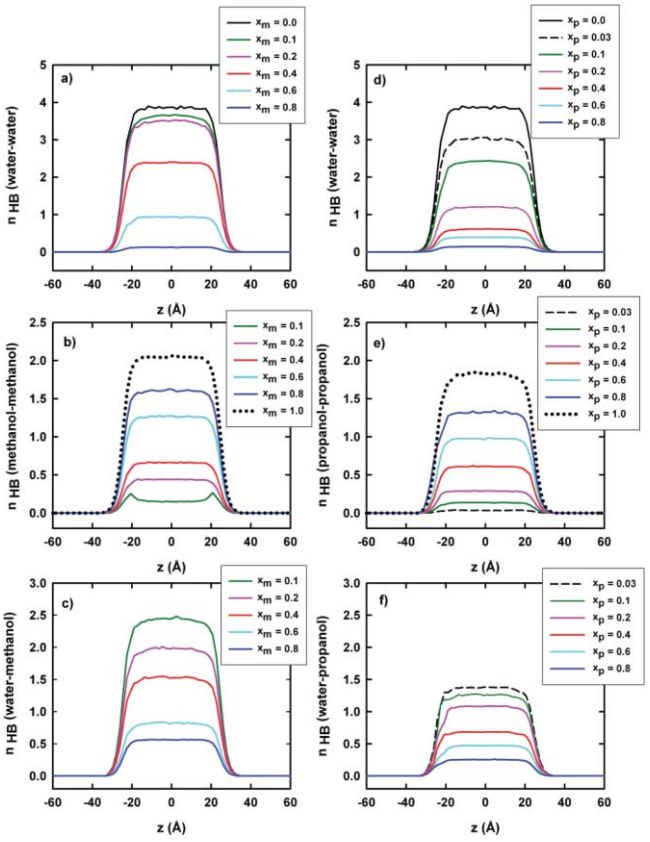

FIG. 5. Profiles of the hydrogen bonds between water–water, alcohol–alcohol, and water–alcohol molecules at 298 K in the (a), (b), and (c) water–methanol mixtures, respectively, and (d), (e), and (f) water-propan-1-ol mixtures at different alcohol mole fractions.

13.1 mN m^{-1}. For completeness, the average methanol–methanol interaction is −25 kJ mol^{-1} including −3 and −22 kJ mol^{-1} for the dispersion-repulsive and electrostatic energy contributions, respectively. The analysis of these contributions in pure solutions shows that the association of methanol molecules through hydrogen bonds is less enthalpically favorable than that of water molecules in line with the fact that water is a highly polar structured liquid. When an alcohol is mixed with water, new alcohol–water (cross association) interactions occur. Depending on the length of the alkyl chain, the mixing can induce the formation of more hydrogen bonds and the change in the existing water–water and alcohol–alcohol hydrogen bonds. As a result, the excess enthalpy of mixing[60] can be positive or negative over the alcohol concentration range.

We complete the molecular description of the water–alcohol mixtures by calculating the profiles of the hydrogen bonds between water–water, water–alcohol, and alcohol–alcohol molecules along the normal to the surface. These profiles are shown in Fig. 5 as a function of the alcohol amount. We use the geometric definition for a hydrogen bond that requires that the oxygen–oxygen distance to be less than 3.5 Å and the H–O···O angle to be less than 30°. Previous studies replaced the angle criterion by a distance criterion.[4,34,46] We take the route of using the angle criterion to be in line with our previous simulations on water–methane[29] and water–CO_2[30] binary mixtures. The number of hydrogen bonds between water molecules in the water–methanol liquid bulk phase decreases from 3.9 to 0.2 [see Fig. 5(a)] when the methanol mole fraction increases from 0 to 0.8. When propanol is mixed with water with a mole fraction of 0.1, we observe in Fig. 5(d) a deep decrease of the average number of hydrogen bonds between water molecules from 3.9 (pure water) to 2.4. For the same amount of methanol ($x_m = 0.1$), the number of hydrogen bonds is 3.7. For a very low amount of propanol (3%), the number of water–water hydrogen bonds is reduced by 25% with respect to pure water.

Figure 5(b) shows the profiles of the average number of methanol–methanol hydrogen bonds as a function of the methanol concentration. In pure methanol, we find an average hydrogen bonds number of 2.05 which matches very well with previous calculations.[34,46] In the case of pure propanol [Fig. 5(e)], the average hydrogen number is close to 1.9. From comparison between Figs. 5(b) and 5(e), we observe that the degree of hydrogen bonding through alcohol molecules in water–methanol solution is larger than that in water–propanol solution.

Figs. 5(c) and 5(f) present the profiles of the water–alcohol hydrogen bonds for methanol and propanol mixtures, respectively. The total number of hydrogen bonds, summing the water–water, water–methanol, and methanol–methanol hydrogen bonds calculated from the average over the slabs in the liquid phase, decreases from 6.4 to 2.4 as the methanol mole fraction increases from 0.1 to 0.8. It means that the degree of hydrogen bonding for mixtures rich in water is larger than that of pure water. For mixtures rich in methanol, the total number of hydrogen bonds is also larger than that of pure methanol. As a result, the excess heat of mixing is negative in the whole methanol concentration range.[60] But, this

does not explain the decrease of the surface tension with increasing methanol amount. The decrease of water–methanol interfacial tension with the methanol concentration can only be interpreted by the decrease of the water–water hydrogen bond over the methanol concentration range. The energy loss in the water–water interaction which is the strongest interaction in the mixture is not then compensated by additional water–methanol and methanol–methanol interactions.

The comparison between the water–methanol and water–propanol mixtures underlines that the number of hydrogen bonds between water and alcohols is halved in propanol solution. The total number of hydrogen bonds in mixtures rich in water is less than that in pure water. As a consequence, the experimental excess enthalpy of mixing for mixtures of water and propanol is less negative and becomes positive for mixtures rich in propanol.[60] Provided that the water–water hydrogen bonds are the strongest from an energy viewpoint, the deep decrease of the surface tension of the water–propanol at low propanol mole fraction is also reflected in Fig. 5(d) by a strong decrease of the number of water–water hydrogen bonds. Additionally, the fact that the number of water–water and water–propanol hydrogen bonds is smaller in mixtures of water and propanol explains why the water–methanol interfacial tension is larger than that of the mixture of water with propanol at low alcohol concentration.

These observations are in line with the fact that water is a highly structured liquid with a three dimensional tetrahedral hydrogen bond network resulting in a relative strong surface tension. In contrast, alcohols are associated liquids in which molecules form winding chains.[1,2] The surface tension of the liquid–vapor equilibrium of this alcohol solution is then smaller with respect to that of water. The addition of alcohol in water breaks the hydrogen bond network and causes the decrease of the interfacial tension of the liquid–vapor interface of the mixture. The decrease of the surface tension of the water–alcohol mixture with the alcohol concentration is found to be predominantly correlated with the decrease of the water–water hydrogen bonds. Indeed, the number of water–water hydrogen bonds in mixtures with 3% of propan-1-ol would correspond to the hydrogen bond number found in water–methanol mixtures with methanol proportions close to 30%: in these two systems with these alcohol amounts (see Tables III and IV), the surface tensions are very close. The number of hydrogen bonds between water molecules in the water–alcohol mixture is found to decrease with increasing the alkyl chain of the alcohol. This explains the dependence of the decrease of the surface tension of water–alcohol mixtures with alcohol chain lengths.

IV. CONCLUSIONS

The Monte Carlo simulations of the water–alcohol liquid vapor interfaces have been performed using the TIP4P/2005 and AUA4 models for water and alcohol, respectively. The main objective is the prediction of the dependence of the water–alcohol surface tension on the alcohol concentration by molecular simulation. The prediction of the interfacial tension as a function of the alcohol composition has been obtained in very good agreement with the experimental data for the water–methanol and water–propanol mixtures. The mechanical and thermodynamic routes used for the surface tension calculation give consistent results. As a consequence, the calculation of the surface tension constitutes a genuine prediction for these force fields because the parameters of these potentials have not been optimized using values of surface tensions. It also shows the transferability of these potentials for mixtures.

The simulations are able to reproduce the deep decrease of the surface tension at small amounts of propanol in water and a more gradual decrease of the surface tension with methanol concentration. The excess surface tension of the water–methanol and water–propanol mixtures are well predicted underlining that the cross interactions are accurately considered through the different potentials and mixing rules.

The deep decrease of the surface tension can be associated at a molecular level with a preferential adsorption of the alcohol molecule at the interface and a decrease of the number of water–water hydrogen bonds in the liquid phase. At low alcohol concentrations, the alcohol molecules prefer to adsorb at the liquid–vapor interface to favor the hydrophobic interactions. At high alcohol concentrations, the hydrophobic interactions are preserved through the formation of winding polymeric chains. The balance between the formation/breaking of hydrogen bonds upon addition of alcohol in water has been discussed in terms of energy. A correlation has been found between the decrease of the number of water–water hydrogen bonds and that of the interfacial tension.

ACKNOWLEDGMENTS

The authors would like to acknowledge the support of the French Agence Nationale de la Recherche (ANR), under grant SUSHI (Grant No. ANR-07-BLAN-0268) “SimUlation de Systèmes Hétérogènes et d’Interfaces.” This work was also granted access to the HPC resources of IDRIS under the allocation 2010-i2010092119 made by GENCI (Grand Equipement National de Calcul Intensif).

[1] A. Laaksonen, P. G. Kusalik, and I. M. Svishchev, J. Phys. Chem. A **101**, 5910 (1997).
[2] S. A. Patel and C. L. Brooks III, J. Chem. Phys. **123**, 164502 (2005).
[3] A. Morita, Chem. Phys. Lett. **375**, 1 (2003).
[4] T. M. Chang and L. X. Dang, J. Phys. Chem. B **109**, 5759 (2005).
[5] F. Biscay, A. Ghoufi, F. Goujon, V. Lachet, and P. Malfreyt, J. Chem. Phys. **130**, 184710 (2009).
[6] A. Ghoufi, F. Goujon, V. Lachet, and P. Malfreyt, Phys. Rev. E **77**, 031601 (2008).
[7] F. Biscay, A. Ghoufi, F. Goujon, V. Lachet, and P. Malfreyt, J. Phys. Chem. B **112**, 13885 (2008).
[8] F. Biscay, A. Ghoufi, V. Lachet, and P. Malfreyt, Phys. Chem. Chem. Phys. **111**, 6132 (2009).
[9] P. Orea, J. Lopez-Lemus, and J. Alejandre, J. Chem. Phys. **123**, 114702 (2005).
[10] M. Gonzalez-Melchor, P. Orea, J. Lopez-Lemus, F. Bresme, and J. Alejandre, J. Chem. Phys. **122**, 094503 (2005).
[11] J. R. Errington and D. A. Kofke, J. Chem. Phys. **127**, 174709 (2007).
[12] A. Trokhymchuk and J. Alejandre, J. Chem. Phys. **111**, 8510 (1999).
[13] J. Lopez-Lemus and J. Alejandre, Mol. Phys. **100**, 2983 (2002).
[14] F. Goujon, P. Malfreyt, A. Boutin, and A. H. Fuchs, J. Chem. Phys. **116**, 8106 (2002).
[15] P. Grosfils and J. F. Lutsko, J. Chem. Phys. **130**, 054703 (2009).
[16] F. Goujon, P. Malfreyt, J. M. Simon, A. Boutin, B. Rousseau, and A. H. Fuchs, J. Chem. Phys. **121**, 12559 (2004).

[17]C. Ibergay, A. Ghoufi, F. Goujon, P. Ungerer, A. Boutin, B. Rousseau, and P. Malfreyt, Phys. Rev. E **75**, 051602 (2007).
[18]F. Goujon, C. Bonal, and P. Malfreyt, Mol. Simul. **35**, 538 (2009).
[19]G. J. Gloor, G. Jackson, F. J. Blas, and E. de Miguel, J. Chem. Phys. **123**, 134703 (2005).
[20]M. Guo and B. C. Y. Lu, J. Chem. Phys. **106**, 3688 (1997).
[21]V. K. Shen, R. D. Mountain, and J. R. Errington, J. Phys. Chem. B **111**, 6198 (2007).
[22]F. Goujon, P. Malfreyt, A. Boutin, and A. H. Fuchs, Mol. Simul. **27**, 99 (2001).
[23]J. Janecek, H. Krienke, and G. Schmeer, Condens. Matter Phys. **10**, 415 (2007).
[24]C. Nieto-Draghi, P. Bonnaud, and P. Ungerer, J. Phys. Chem. C **111**, 15686 (2007).
[25]J. Alejandre, D. J. Tildesley, and G. A. Chapela, J. Chem. Phys. **102**, 4574 (1995).
[26]C. Vega and E. de Miguel, J. Chem. Phys. **126**, 154707 (2007).
[27]A. Ghoufi, F. Goujon, V. Lachet, and P. Malfreyt, J. Chem. Phys. **128**, 154716 (2008).
[28]A. Ghoufi, F. Goujon, V. Lachet, and P. Malfreyt, J. Chem. Phys. **128**, 154718 (2008).
[29]F. Biscay, A. Ghoufi, V. Lachet, and P. Malfreyt, J. Chem. Phys. **131**, 124707 (2009).
[30]F. Biscay, A. Ghoufi, V. Lachet, and P. Malfreyt, J. Phys. Chem. B **113**, 14277 (2009).
[31]W. L. Jorgensen, J. D. Madura, and C. J. Swenson, J. Am. Chem. Soc. **106**, 6638 (1984).
[32]J. I. Siepmann, Nature **365**, 330 (1993).
[33]M. E. V. Leeuwen, Mol. Phys. **87**, 87 (1996).
[34]B. Chen, J. Potoff, and J. I. Siepmann, J. Phys. Chem. B **105**, 3093 (2001).
[35]J. M. Stubbs, J. J. Potoff, and I. J. Siepmann, J. Phys. Chem. B **108**, 17596 (2004).
[36]S. Toxvaerd, J. Chem. Phys. **93**, 4290 (1990).
[37]S. Toxvaerd, J. Chem. Phys. **107**, 5197 (1997).
[38]P. Ungerer, C. Beauvais, J. Delhommelle, A. Boutin, B. Rousseau, and A. Fuchs, J. Chem. Phys. **112**, 5499 (2000).
[39]E. Bourasseau, P. Ungerer, A. Boutin, and A. H. Fuchs, Mol. Simul. **28**, 317 (2002).
[40]E. Bourasseau, M. Haboudou, A. Boutin, A. H. Fuchs, and P. Ungerer, J. Chem. Phys. **118**, 3020 (2003).
[41]M. G. Ahunhay, J. Perez-Pellitero, R. O. Contreras-Camacho, J. M. Teuler, P. Ungerer, and V. Lachet, J. Phys. Chem. B **109**, 2970 (2005).
[42]R. O. Contreras-Camacho, P. Ungerer, M. G. Ahunbay, V. Lachet, J. Perez-Pellitero, and A. D. Mackie, J. Phys. Chem. B **108**, 14115 (2004).
[43]R. O. Contreras-Camacho, P. Ungerer, A. Boutin, and A. D. Mackie, J. Phys. Chem. B **108**, 14109 (2004).
[44]P. Bonnaud, C. Nieto-Draghi, and P. Ungerer, J. Phys. Chem. B **111**, 3730 (2007).
[45]C. Nieto-Draghi, P. Bonnaud, and P. Ungerer, J. Phys. Chem. C **111**, 15942 (2007).
[46]N. Ferrando, V. Lachet, J. M. Teuler, and A. Boutin, J. Phys. Chem. B **113**, 5985 (2009).
[47]L. X. Dang and T. M. Chang, J. Chem. Phys. **106**, 8149 (1997).
[48]L. X. Dang and T. M. Chang, J. Chem. Phys. **119**, 9851 (2003).
[49]J. L.F. Abascal and C. Vega, J. Chem. Phys. **123**, 234505 (2005).
[50]See supplementary material at http://dx.doi.org/10.1063/1.3544926 for a description of the potential models of water and alcohols.
[51]L. R. Dodd, T. D. Boone, and D. N. Theodorou, Mol. Phys. **78**, 961 (1993).
[52]J. S. Rowlinson and B. Widom, *Molecular Theory of Capillarity* (Clarendon Press, Oxford, 1982).
[53]J. G. Kirkwood and F. P. Buff, J. Chem. Phys. **17**, 338 (1949).
[54]J. H. Irving and J. G. Kirkwood, J. Chem. Phys. **18**, 817 (1950).
[55]J. P. R. B. Walton, D. J. Tildesley, J. S. Rowlinson, and J. R. Henderson, Mol. Phys. **48**, 1357 (1983).
[56]J. P. R. B. Walton and K. E. Gubbins, Mol. Phys. **55**, 679 (1985).
[57]M. Gonzalez-Melchor, F. Bresme, and J. Alejandre, J. Chem. Phys. **122**, 104710 (2005).
[58]J. Alejandre and G. A. Chapela, J. Chem. Phys. **132**, 014701 (2010).
[59]J. L. Rivera, C. McCabe, and P. T. Cummings, Phys. Rev. E **67**, 011603 (2003).
[60]R. F. Lama and B. C.Y. Lu, J. Chem. Eng. Data **10**, 216 (1965).
[61]G. Vasquez, E. Alvarez, and J. M. Navaza, J. Chem. Eng. Data **40**, 611 (1995).